Proceedings of the ASME 2017 36th International Conference on Ocean, Offshore and Arctic Engineering
OMAE2017
June 25-30, 2017, Trondheim, Norway

OMAE2017-61042

REAL-TIME HYBRID TESTING OF THE HYBRID POWER PLANT: CONCEPT AND FEASIBILITY TEST

Kevin Koosup Yum
Sintef Ocean*
Trondheim, Norway
Email: kevinkoosup.yum@sintef.no

ABSTRACT

Concept of the real-time hybrid testing framework for marine hybrid power plant is presented. The benefits and challenges with regard to using the model-scale power plant for the testing are explained. As a feasibility study of the methodology, tests are performed at the Hybrid Power Laboratory with a model-scale physical diesel-electric power plant. In this test, a load profile from onboard measurements from a ship is used as a numerical part of the system. In the model-scale power plant, the electrical part of the plant is used as an actuator to generate the load for the diesel engine. The traceability of the components and the total system to the given load profile is quantified in terms of time delay and tracking errors. For conclusion, the limitation of the test is analyzed and suggestions for improving the results are provided.

NOMENCLATURE

HPL Hybrid Power Laboratory
ESD Energy Storage Device
AC Alternative current
DC Direct current

[1]Norwegian Marine Technology Research Institute (MARINTEK) and SINTEF Fisheries and Aquaculture are merged into a new private limited company, SINTEF Ocean, operative from 1 January 2017. The department for environmental technology in SINTEF Material and Chemistry will also be transferred to the new company.

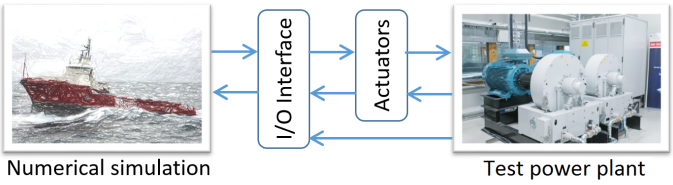

FIGURE 1: Hybrid testing setup for a marine power system

INTRODUCTION

Validation of a system and control design for a hybrid power system is a challenging task. In a hybrid power plant for marine application, an energy storage device (ESD) such as batteries, super-capacitors, flywheels, etc., are included. It adds flexibility to operation of a power plant, which can be exploited to enhance efficiency of the system, to increase the safety and to reduce the running hours of the machineries. On the other side, it adds complexity to the system, which has to be properly handled by a high-level controller: power and energy management system. A real-time hybrid testing framework can provide capability to test the complex system with realistic load under a controlled environment. In this framework, one or more parts of the target system are replaced by numerical simulations while the rest of the system is physically tested. The numerical part of the system should be connected to the physical part by a proper actuator. The system may be closed-loop or open-loop depending on the degree of coupling between the numerical part and the physical one. Figure 1 shows a schematic diagram of such a setup.

The term, hybrid testing, is used in different names according to the areas of applications. In earthquake engineering in which the concept of the hybrid testing was first introduced and applied [1], it is referred as real-time hybrid testing from which the name is borrowed in this paper. In the mechanical engineering, it is often called a model-in-the-loop test [2]. In the study of electrical system, this approach has been applied to test the specific components of power electronics [3, 4], the control systems or electro-mechanical machines at reduced scale [5]. The methodology is referred as power level hardware-in-the-loop (PHIL) simulation or mechanical level hardware-in-the-loop (MHIL) simulation [6]. Finally, the group from SINTEF Ocean and Norwegian Univerisity of Science Technology, developing offshore wind turbine technologies has come up with the fully dynamic hybrid testing, which they named as Real-Time Hybrid Model Testing or ReaTHM [7]. The set-up in Figure 1 can be referred as MHIL simulation, but the system in the hardware model is more complex than studied in the literatures.

CONCEPT AND DESIGN OF THE REAL-TIME HYBRID TESTING FOR THE MARINE POWER PLANT

What is fundamentally different in this paper from the previous work is to use a scaled power plant including the prime movers, diesel engines. Including the diesel engines enables us to measure actual fuel consumption and emissions, which are difficult to estimate when the load is highly transient. In addition, often the response of the plant is determined at the diesel engine as the diesel engine has slower dynamics than the electrical system in general. Therefore, it is possible to put the physical constraint for the possible load changes on the gensets. However, using the full system set-up imposes challenges in terms of controllability as the degree of the freedom is wider and stiffness in terms of configuration and scaling since it is difficult to change the system setup or capacity of the each machinery.

The main objectives of this work is to verify the relevance and feasibility of the hybrid model testing method for the marine power plant using the Hybrid Power Laboratory (HPL). In terms of relevance, the test method should provide benefits compared to other alternatives. Other alternatives can be a sequential test in a open-loop fashion where the input to the test is simulated in the numerical simulation and then fed to the experimental set-up. When the external load is close to the steady state case or when the coupling between the numerical simulation part and the physical plant part is weak, this type of a test may be good enough.

For feasibility of the test, following limitation of the test should be addressed:

Running tests are costly so minimum scope and time are preferred

The testing facilities are more/less fixed. If the desired power plant or its configuration differs from the facility, compensation should be done by on-line scaling or compensation by additional simulations.

The power plant, as a complex system, may have internal dynamics that are not controllable or unidentified.

As the configuration and capacity of the main components in HPL are fixed or difficult to change, the power plant of the target vessel should be scaled or reconfigured so that the facility can accommodate the test cases. Cases that demand scaling or reconfiguration of the power system can be addressed as follows:

- The capacities of the components in the real plant differ by an order of magnitude,
- The system of the real plant differ in nature: e.g., AC vs. DC, gas engine vs. diesel engine, mechanical drive vs. diesel electric,
- A part of the real plant is missing in the test plant,
- The real plant has more gensets,
- The real plant has more thrusters.

In these cases mentioned above, the power plant in the laboratory cannot represent the actual plant as is, and modification should be made to the inputs of the test. A list of options for the modifications are listed as follows:

- Scale the input to the test plant by a pre-set ratio,
- Aggregate similar inputs to one,
- Use simulations for a part of the power plant,
- Use simulation or conversion tool to convert the dynamics of the input.

In general, a marine system follows scaling law by Froude number in which the speed and the length are scaled according to the following equation:

$$\frac{u_{\mathrm{FS}}}{gl_{\mathrm{FS}}} = \frac{u_{\mathrm{MS}}}{gl_{\mathrm{MS}}} \tag{1}$$

where u is speed, g is gravitational acceleration and l is a characteristic length. The subscript FS stands for full scale whereas MS stands for model scale. Given the model scale in the main dimension, 1:x, the following similitude laws can be withdrawn:

Similitude of velocity $\rightarrow 1 : \sqrt{x}$
Similitude of time $\rightarrow 1 : \sqrt{x}$
Similitude of force $\rightarrow 1 : x^3$
Similitude of power $\rightarrow 1 : x^{7/2}$

Figure 2 shows the relationship between the power scale and the length or time scale. In the hybrid power lab, the two electric motors consume 400kW at maximum. For the power scale 1:100, which means 40MW in the power consumption in full scale, the length scale is 3.73 and the time scale is 1.93. Therefore, the

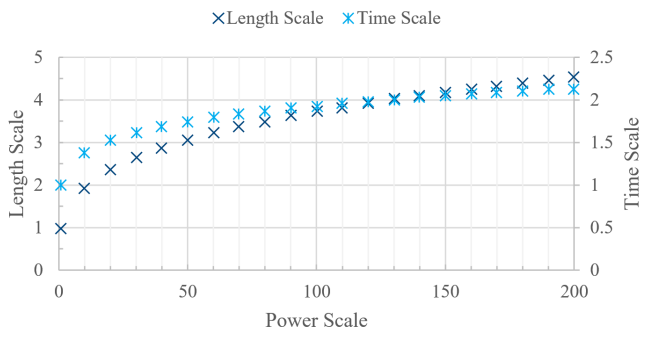

FIGURE 2: Power scale vs. length and time scale for Froude scaling

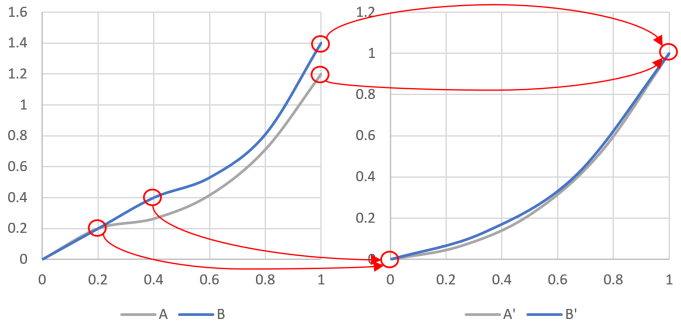

FIGURE 3: Mapping of the real plant to the test plant

simulation time should be at most two times faster than the real time, which is quite feasible for the current vessel simulator.

The scaling ratio can be determined in several ways. The simplest way is to apply the ratio of rated power of the real power plant to the test plant. As the components could have different ratios, the component having the largest ratio should determine the overall ratio, assuming the real plant is greater. If the outputs of the real and test plant are highly nonlinear, the scaling can be done in the ranges in which they show similar behaviors to capture the nonlinearity of the system. For example, in Figure 3, a curve for an output variable against an input variable is given for the real plant (A) and the test plant (B). We can observe that the output of A has a linear relation with the input up to 0.2 and a nonlinear relation above. For B, the nonlinear range of input is from 0.4 and above. The points at lower limit (0.2 and 0.4 for A and B, respectively) can then be mapped to an identical point, and the points at upper limit of the nonlinearity can be mapped to another identical point. In this way, the test plant is scaled so that the nonlinearity is conserved.

When there are more gensets or power producers, one can aggregate input for the similar components. For example, when you have 2 x 1000kW + 2 x 500 kW gensets, we may assume 1 x 2000 kW + 1 x 1000 kW configuration by summing the inputs for the engines with the same capacity, provided that the load is shared by all gensets. However, it results in inappropriate scaling if the gensets are asymmetrically loaded or there is an off-line genset.

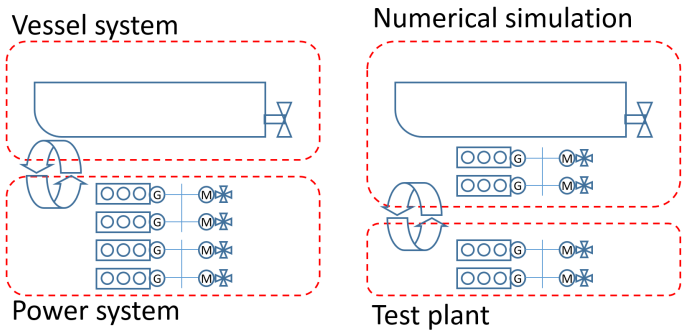

FIGURE 4: Boundary for the systems and for the hybrid testing

Depending on the availability, a mathematical model may replace a part of the power plant. In the hybrid testing set-up, this is done by adjusting the boundary between the numerical simulation and the testing component. As shown on the left in Figure 4, it would be natural to put the boundaries between the vessel system and the power system when designing the hybrid testing set-up. However, we may adjust this boundary so that only a part of the power system is tested while the rest is simulated numerically with the vessel system.

FEASIBILITY TEST

One of the biggest challenges with the hybrid testing in general is the stability of the whole system induced by the delays at the actuators. Moreover, the design of the test depends on the dynamics of the actuators and their configurations. Therefore, it is important to understand the dynamics of the whole system as well as its components.

There exists a number of possibilities of configuring the laboratory power plant for the real-time hybrid model testing. The current setup of the Hybrid Power Laboratory (HPL) at Sintef Ocean is shown in Figure 5. In the configuration, there are two types mechanical interfaces between components: one between the diesel engines and the generators (hereafter called DG interface) and the other between the electric motor and the brake (hereafter called EM interface). Both of the mechanical interfaces can be utilized as the interface with the numerical simulation for hybrid testing.

In case of using DG interface for hybrid testing, the total electric power plant can be used as an actuator (see Figure 2 on the left side). The power on the generator or the torque can be controlled by the brake, battery and capacitor depending on the characteristics of the load. If the load is slow varying and highly

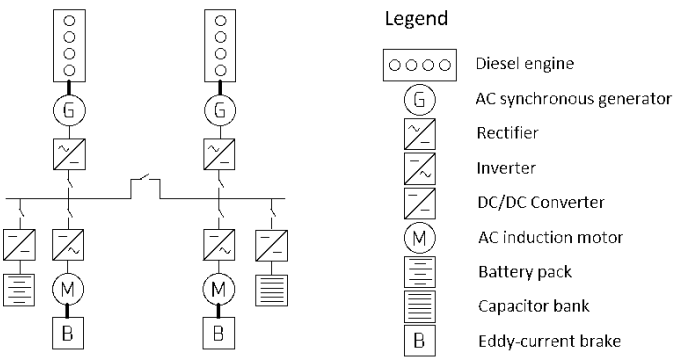

FIGURE 5: Single line diagram of the Hybrid Power Lab

biased, brakes can be mainly used to provide the load on the system. On the other hand, the energy storage devices (ESD) can generate loads that are highly transient and have low mean value. When the load is highly transient and has a significant mean value, the brake and the ESDs can be coordinated where the brake provides the slow-varying mean load whereas the ESD takes the rest of the load. In this test setup, a mechanical response of the diesel engine, the fuel consumption and the emissions will be of interest.

For the EM interfaces, the eddy-current brake on the electric motors as the main actuator for the test (see Figure 2 on the right side). This configuration can also be used for testing the real plant with both the mechanical drive and the electrical drive. For the mechanical drive simulation, the response of the electric motor should be tuned to match the dynamics of a diesel engine by adjusting the speed regulator.

As various configurations and a number of different controllable devices are available, it is important to understand the dynamics of the overall systems and the individual components in order to design the experiment utilizing most of the potentials of the available facility. In this regard, an introductory test was performed in order to discover the dynamics of the system and devices for the given control inputs.

The purpose of the tests are:

- Demonstrate the feasibility of running the hybrid testing of the power plant
- Demonstrate and quantify the dynamics or delays of the actuators for the load profile with different degrees of transiency.
- Demonstrate and quantify the dynamics or delays of the actuators for the load profile with different configuration of the actuators.

Test procedure and configuration

The test procedure and the configuration is summarized in Figure 6. In this introductory test, the measured load profiles

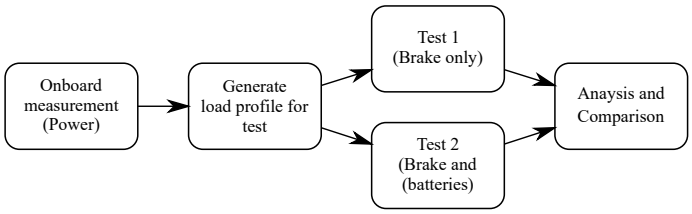

FIGURE 6: Test procedure and configuration

are used instead of numerical simulation of the vessel. The test is performed in the open loop where there is no feedback to the numerical substructure. The response of the system (power load at the generator and the diesel engine) is measured and compared to the desired load to quantify the delay and the tracking errors. For actuators, two different configurations will be tested: one with only brakes and the other with coordination of brakes and batteries.

Load profiles for the test

The given load profile data from onboard measurement are slowly varying signal for it has been smoothed by moving average with a 30 second interval. In the real world, the load will have more fluctuations at higher frequencies, and the effect of such fast changing loads on the machineries are interesting. Therefore, artificial noises are added to the given signal, which emulates realistic loads.

In order to generate the random noises, the given data are first resampled at the sampling rate of the test control system, 10 Hz, by interpolation. The sampled data set is called X. Then, three frequencies are selected for the random noise components (1, 0.3, 0.05 Hz). For each frequency component, the Gaussian white noise is calculated and added to the original data. The noise is calculated according to the following equation:

$$w_i' = \sqrt{\frac{\sum_{i=1}^{N'} \|x_i'\|^2}{N' SNR}} u, \quad u \sim \mathcal{N}(0,1) \tag{2}$$

where, x_i' is an element of X' which is a set of sampled from X with the noise frequency, N' is the number of elements in the set X', SNR is a signal-to-noise ratio, and u is a random number from the normal distribution. The parameters in Table 1 are used for different cases in order to generate the load profile with various levels of transiency. Figure 7 shows the generated load profile with noises from the given load profiles from case 1 to 4 in the descending order from the top.

Configuration of the test

Not all the operation modes can be tested in the given configuration, nor are they interesting. The feasible test set up with the

TABLE 1: Noise characteristics for the power load profile

	High frequency noise		Medium frequency noise		Low frequency noise	
	Freq. (Hz)	Amp (dB)	Freq. (Hz)	Amp (dB)	Freq. (Hz)	Amp (dB)
Case 1	1	25	0.3	22	0.05	23
Case 2	1	30	0.3	27	0.05	28
Case 3	1	35	0.3	32	0.05	33
Case 4	1	50	0.3	50	0.05	50

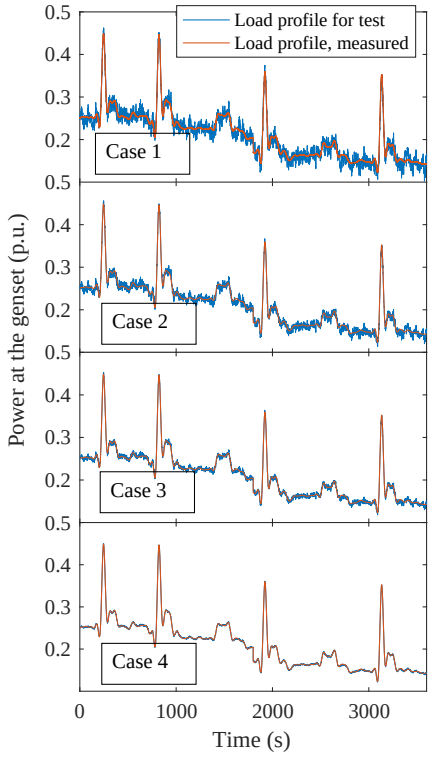

FIGURE 7: Load profiles of the generator with artificial noises

available measurements to have the diesel gensets as the physical substructure. In the test plant, the whole power plant before the generators can be used as actuators. Both the brakes and the ESDs can be used to produce the desired load from the measurement. In the test, the feasibility and the effect of using only brakes and both brakes and ESDs are both tested, and the results are compared.

In the first test in which only brakes are used as actuators, the load profiles generated are given in power and, therefore, have to be converted to torque. For the conversion, power ratio of the

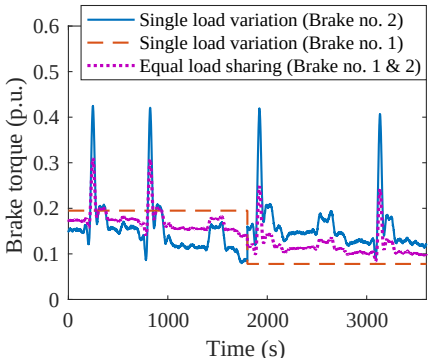

FIGURE 8: Reference torque on the brakes for the test

generators between the real power plant and the test plant has to be considered. In addition, as we are interested in the load on the genset, the conversion efficiencies from the brake to the generator should be considered. We assume constant efficiencies despite they change over different operational conditions. It is also assumed that the electric motor connected to the brakes run at a constant speed, 1500 RPM. As two brakes are used to generate the load, there are two different operational modes to do so: one is to provide the identical loads from both of the brakes, and the other is one brake providing a constant load while the other is providing the rest of the power. We refer the former mode as equal load sharing and the latter as single load variation. Then the reference torque on each brake can be calculated as following:

$$\begin{aligned} &\text{Equal load sharing:} && Q_{\text{brake1,2}} = \frac{P_L}{2N}\frac{P_{\text{rate,test}}}{P_{\text{rate,real}}}\frac{1}{\eta} \\ &\text{Single load variation:} && Q_{\text{brake1}} = const \\ & && Q_{\text{brake2}} = \frac{P_L}{N}\frac{P_{\text{rate,test}}}{P_{\text{rate,real}}}\frac{1}{\eta} - Q_{\text{brake1}} \end{aligned} \tag{3}$$

where N is the rotational speed of the motor in rad/s, P_L is the reference load, $P_{\text{rate,test}}$ is the rated power of the diesel engine in the lab, $P_{\text{rate,real}}$ is the rated power of the diesel engine in the real vessel, η is the total efficiency from the shaft of the brake to the genset. Figure 8 shows the calculated reference torques. Both modes will be tested and compared.

In the second test, batteries can be used to provide the fast transient part of the load whereas the brake can provide the slow varying part. It is also important that the state of charge of the battery stay within the allowable limits. The loads on the brakes are manually adjusted to meet both requirements, as shown in Figure 9. Note that the power of the battery is positive when it discharges, or generates power in other words, and negative when it charges. Therefore, the reference values for the power always satisfies the following relation:

$$P_{\text{ref}} = P_{\text{ref,brakes}} - P_{\text{ref,Battery}} \tag{4}$$

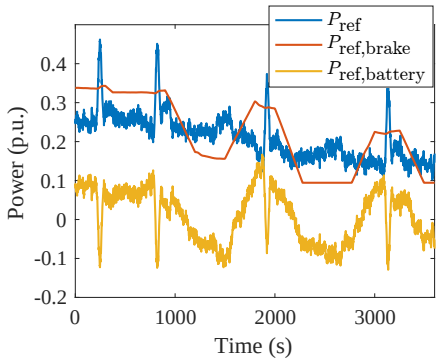

FIGURE 9: Load profile of the test with the brakes and the batteries

The specifications for the test facilities are given in Table 2.

TABLE 2: Particulars for the engine test bench

	Capacity	Type
Diesel engines	209kW, 412kW	Perkins 2506-E15TAG1 Turbocharged, 6 cylinder inline, Generator engine
Electric motors	200kW	Induction motor
Generators	230kVA, 400kVA	Synchronous, variable speed
Brake	470kW	Horiba WT-470 Eddy current
Battery pack	Discharge 300A, Charge 150A	Lithum ion
Main bus voltage	540V DC	
Data acquisition system	10Hz	Labview with NI cRIO

RESULT AND ANLYSIS

The result and the analysis of the test are presented to identify the quantity and trends of time delay and tracking error in the brakes, the batteries, the electric plant and the total system in terms of response to the reference signals. The main interested output of each test is the delays of the torque and power compared to the reference signal and the tracking error. First, the tracking error is defined as:

$$e = \frac{\sum_{i=1}^{N} \left(X_{i,\text{ref}} - X_{i+L,\text{meas}}\right)^2}{N} \tag{5}$$

where, $X_{i,\text{ref}}$ is the i^{th} sample of a reference signal in the range of interest, N is the number of the samples in the range and $X_{i+L,\text{meas}}$ is the i^{th} sample of the measured signal where L is the index corresponding to the time delay. L is calculated as following:

$$L = \frac{t_d}{f_{\text{samp}}} \tag{6}$$

where t_d is the time delay in seconds, and f_{samp} is the sampling frequency. The time delay is determined so that the tracking error become the minimum value.

Load Generated by the Brakes Only

In the test with using only brakes to generate load on the genset, we can identify the dynamics of the brake and the whole system separately. The results are analyzed for two separate time intervals as shown in Table 3. The main difference between the two intervals are the mean power load level. The average power is 0.33 p.u. for the first interval and 0.21 p.u. for the second.

TABLE 3: Time intervals for the analysis of the result

Starting time (s)	Ending time (s)	Torque profile
200	1600	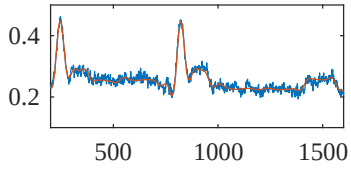
2000	3400	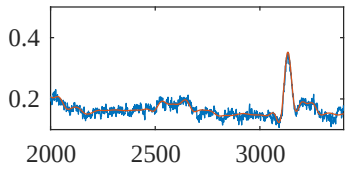

From the test, it was found that there is a slightly more delay for the equal load sharing compared to the single load variation for the torque response ahs shown in Figure 10. The time delay is consistently lower for the single load variation. Moreover, the delay is increasing as the reference load becomes less transient (less noise). This trend is similar for the first brake.

Regarding the delay in the electrical system by comparing the power at the electric motor shaft to the engine shaft power. The delay is negligible in most of cases for our sampling frequency (10Hz). Therefore, the most of delays are originated from

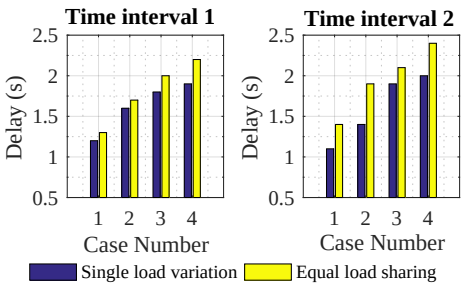

FIGURE 10: Time delay of the second brake in torque

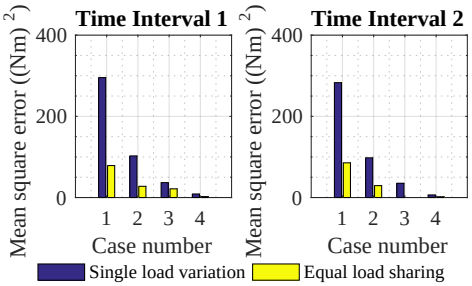

FIGURE 12: Time delay of the battery in power

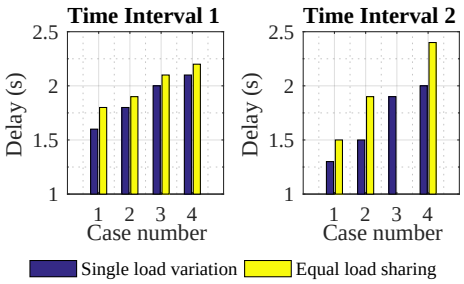

FIGURE 11: Time delay of the total system in power

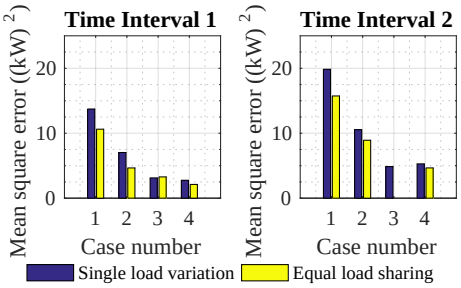

FIGURE 13: Mean square tracking error of the battery

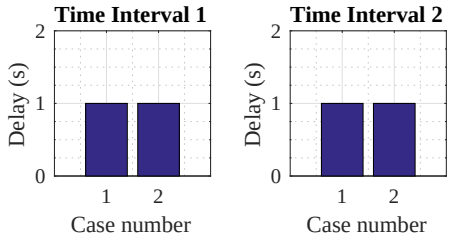

FIGURE 14: Time delay of the battery with regard to power

the brakes, and this delay coincides the delays in the power at the diesel engine from the reference as shown in Figure 11.

In terms of tracking errors, the trend is opposite to the time delay as shown in Figure 12 and 13. The error decreases as the reference signal becomes less transient (less noise), and the single load variation has far greater error than the equal load sharing. Interestingly, the time delay and the tracking error conflict each other in this test. Note that the mean square error at the system level is lower than ones at the brake level. One of the possible reason for it could be measurement noise in the torque signals from the brake which contributes to the increased mean square errors. Another possibility is that the power conversion and transmission through the motor, the generator and the engine shaft could filter the power fluctuations. This must be further investigated.

Load Generated by the Brakes and the Batteries

In this test, the dynamics of the battery and the whole system are identified separately. Likewise, the results are analyzed for two separate time intervals as shown in Table 3. The time delay for the battery and the tracking error are shown in Figure 14 and Figure 15. Interestingly, the delay is always constant, 1 second. From a step load test of the battery, which is out of scope in this work, it was found that this delay is consistent and caused by the communication delay, rather than dynamics of the system. In fact, the dynamics of the battery is found to be too fast to be captured at the sampling rate of the current data acquisition system. In terms of the tracking error, the battery showed superior result with very small errors for even the most transient case.

Regarding the total system response, unlike the brake only cases, the delay and the tracking error showed greater dependence on the time intervals than the load cases (see Figure 16 and Figure 17). As mentioned, the main difference between the time intervals is the mean power level, 137kW and 88.2kW respectively. This trend was however not observed in the first test using brakes only. Furthermore, in spite of the excellent capability of the battery to follow the reference signal, the tracking error remained in the similar level to the brake only cases. We observed that even the battery could follow the load changes happening at 1 Hz frequency, the system response at the shaft of the

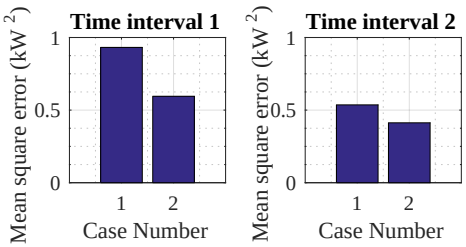

FIGURE 15: Mean square tracking error of the battery with regard to power

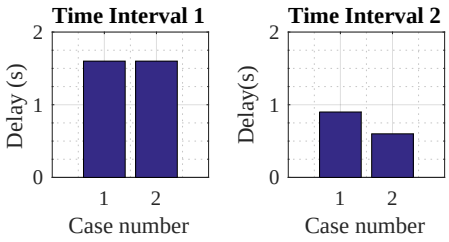

FIGURE 16: Time delay of the total system using batteries with regard to power

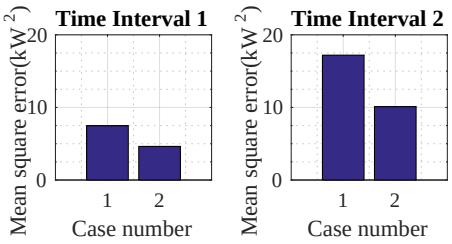

FIGURE 17: Mean square error of the total system using batteries with regard to power

engine does not follow accordingly, as shown in Figure 18. This is one of the main contribution to the error for the power tracking in the total system. Note that the direction of the power for the battery is opposite to the generator's.

There is another source of error that must be taken into account in order to use the total system as an actuator: conversion efficiencies of the individual components. While analyzing the data, the power calculated at the genset shaft had to be multiplied by a factor in order to match the magnitude of the reference power signal. The value of the factor ranges from 0.85 to 0.88. The correction factor accounts for the generator efficiency as well as uncertainties in the other efficiencies that has been accounted for. For the convenience and due to lack of knowledge, we only applied constant efficiencies. However, the actual values vary with the operational conditions, mainly for the power load and speed. This is shown in Figure 19 in which the reference

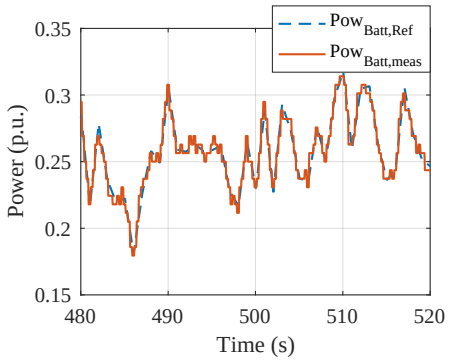

(a) Battery power

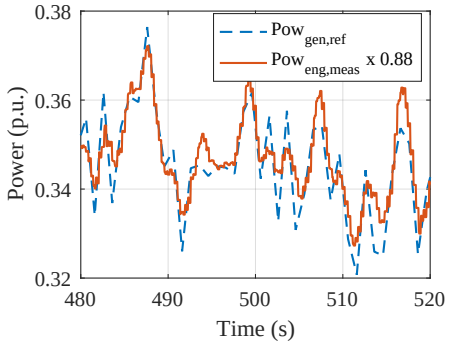

(b) Diesel engine shaft power

FIGURE 18: Time series of power tracking of the battery and the diesel engine for the case 1

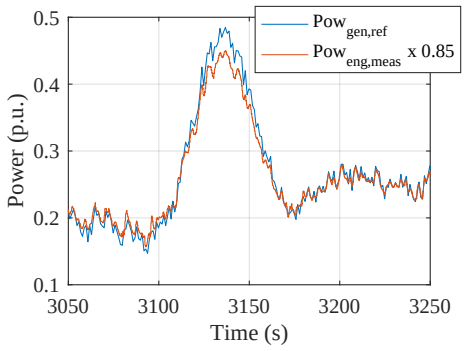

FIGURE 19: Time series of power tracking of the diesel engine for the case 1

is higher at the peak and lower at the bottom than the measurement. This implies that the overall efficiency should be higher than the set value for the high loads and lower for the low loads. Therefore, when converting the reference signal to the command signals for the actuators, variable efficiencies depending on the operational conditions should be applied.

CONCLUSION

In this paper, the concept of the hybrid model testing for a marine hybrid power plant was presented. This test method is a novel concept in the way that a full machinery setup including diesel engines is used instead of a single component or simplified machineries. Possible benefits and challenges are addressed. Furthermore, the feasibility of the power tracking at the diesel engine was carried out using the total electric plant and the available actuators, the brakes and the batteries. The load profiles on the gensets were provided from a onboard measurement, to which noises were added in order to produce more realistic variations in the load in different degrees. The first test was performed without the batteries, and the second test included them to generate a fast-changing part of the load. From the result, the time delays and the tracking errors were quantified for the actuator.

In general, the brakes showed relatively slow response with an average time delay of 1.87 seconds and large errors. Sharing the load with two brakes provided smaller error with longer delay. The batteries showed a very fast dynamic response, beyond the sampling frequency of 10Hz in the test, and accurate load-following capability. However, the communication delay was found to be the bottle-neck in terms of the response. The time delay and the tracking error showed opposite trends when they were compared among cases of various level of transiency or among the different operational modes: single load variation vs. equal load sharing.

The limitation of the test was that it was difficult to find the causes for the findings because of the holistic approach of the test. These findings are the conflicting trends between the time delays and the tracking errors, dependence of the time delays on the mean load level for the second test. If possible in the further work, the delays should be separately identified for communication, for sensors and for each component. In addition, the errors due to the variable efficiencies should be taken into account for generation of the command signal to the actuators.

ACKNOWLEDGMENT

This work is funded by the project 'Hybrid Testing: Real-Time Hybrid Model Testing for Extreme Marine Environments'. The project is financed by the Research Council of Norway's MAROFF program together with the industry.

REFERENCES

[1] Nakashima, M., Kato, H., and Takaoka, E., 1992. "Development of real-time pseudo dynamic testing". *Earthquake Engineering & Structural Dynamics,* ***21***(1), pp. 79–92.

[2] Plummer, A. R., 2006. "Model-in-the-loop testing". *Proceedings of the Institution of Mechanical Engineers, Part I: Journal of Systems and Control Engineering,* ***220***(3), pp. 183–199.

[3] Steurer, M., Edrington, C. S., Sloderbeck, M., Ren, W., and Langston, J., 2010. "A megawatt-scale power hardware-in-the-loop simulation setup for motor drives". *IEEE Transactions on Industrial Electronics,* ***57***(4), pp. 1254–1260.

[4] Letrouve, T., Lhomme, W., and Dollinger, N., 2013. "Control validation of Peugeot 3008 HYbrid4 Vehicle Using a Reduced-scale Power HIL Simulation". *Journal of Electrical Engineering and Technology,* ***8***(5), pp. 1227–1233.

[5] Allegre, A. L., Bouscayrol, A., Verhille, J. N., Delarue, P., Chattot, E., and El-Fassi, S., 2010. "Reduced-scale-power hardware-in-the-loop simulation of an innovative subway". *IEEE Transactions on Industrial Electronics,* ***57***(4), pp. 1175–1185.

[6] Bouscayrol, A., 2008. "Different types of Hardware-In-the-Loop simulation for electric drives". *Industrial Electronics, 2008. ISIE 2008. IEEE International Symposium on*, pp. 2146–2151.

[7] Sauder, T., Chabaud, V., Thys, M., Bachynski, E. E., Sæther, L. O., Ntnu, V. C., and Marintek, M. T., 2016. "Real-Time Hybrid Model Testing of a Braceless Semi-Submersible Wind Turbine: Part IThe Hybrid Approach". In ASME 2016 35th International Conference on Ocean, Offshore and Arctic Engineering, no. 3, American Society of Mechanical Engineers, pp. V006T09A039–V006T09A039.